Integrated lithospheric modelling in the Red Sea area

A. H. A. Radwan, E. A. Issawy
National Research Institute of Astronomy and Geophysics, Department of geodynamics[1]

J. Dérerová
Geophysical Institute of the Slovak Academy of Sciences[2]

M. Bielik
Department of Applied and Environmental Geophysics, Faculty of Natural Sciences, Comenius University[3]
Geophysical Institute of the Slovak Academy of Sciences[2]

I. Kohút
Geophysical Institute of the Slovak Academy of Sciences[2]

A b s t r a c t : The paper is the first attempt to apply 2D integrated geophysical modelling to the determination of the lithospheric structure and its thickness in the Red Sea area. The results show large differences between continental and oceanic lithospheric structure and thickness. The oceanic crust of the Red Sea is much thinner (12-15 km) in comparison with the continental crust which is located on both sides of the Read Sea, and reaches the thickness of around 28-33 km. The density of the lowermost part of the upper mantle in the Red Sea area is very low indicating possible presence of partial melting in the upper mantle and supporting the theory of uplift of the asthenospheric masses in the Read Sea that is accompanied by the process of underplating beneath the Moho discontinuity.

Key words: the Red Sea, integrated modelling, lithospheric thickness, upper mantle

[1] Helwan 11421 El-Marsad St., Cairo, Egypt
e-mail: radwan99@nriag.sci.eg, issawy@nriag.sci.eg
[2] Dúbravská cesta 9, 845 28 Bratislava, Slovak Republic;
e-mail: geofjade@savba.sk
[3] Mlynská dolina, 842 15 Bratislava, Slovak Republic;
e-mail: bielik@fns.uniba.sk

1. Introduction

The Red Sea is considered to be a typical example of a newly formed ocean, therefore a great number of studies discuss its evolution and development especially in relationship to continental rifting, initiation of sea floor spreading and plate tectonics (*Tramontini and Davies, 1969; Makris et al., 1983; Gaulier et al., 1988; Martinez and Cochran, 1988*).

The paper is focused on the 2D integrated geophysical modelling with a goal to calculate an original model of the lithospheric structure and lithosphere thickness along Profile 1 in the Red Sea region. To know the lithospheric structure and thickness is important for geodynamical reconstruction of the area.

2. Geological settings

After *Saleh et al. (2006)*, the oldest known formation in the Read Sea rift region is the igneous and metamorphic rocks of Late Precambrian age (Fig. 1). This type of rocks has formed in the northern edge of the African Shield. In some places of the southern Sinai and in the Eastern Desert (Red Sea mountain range) the Late Precambrian basement complex outcrops. Note that the depth of the basement increases northwards towards the Mediterranean Sea (*Said, 1962* and *El-Gezeery and Marsouk, 1974*). The Palaeozoic rocks are characterized by continental clastic deposits. The marine episodes are minor in space and time. The Palaeozoic period ended with the Upper Carboniferous-Lower Permian marine deposition that followed the Hercynian orogenic phase, and the subsequent erosional period. Predominant continental deposition started again in the Mesozoic (*Saleh et al., 2006*).

Transgression of Middle Triassic marine from the Tethys appears to be limited to the area of northern Sinai and the Gulf of Suez. It is suggested that Jurassic deposits cover parts of the west side of the Gulf of Suez. It seems to be that the distribution of the Jurassic sediments around the Gulf is as far south as Wadi Araba. These sediments include fluvio-marine and marine shallow-water deposits (*El-Gezeery and Marsouk, 1974*). The maximum extension of the sea seems to have occurred during Middle Jurassic

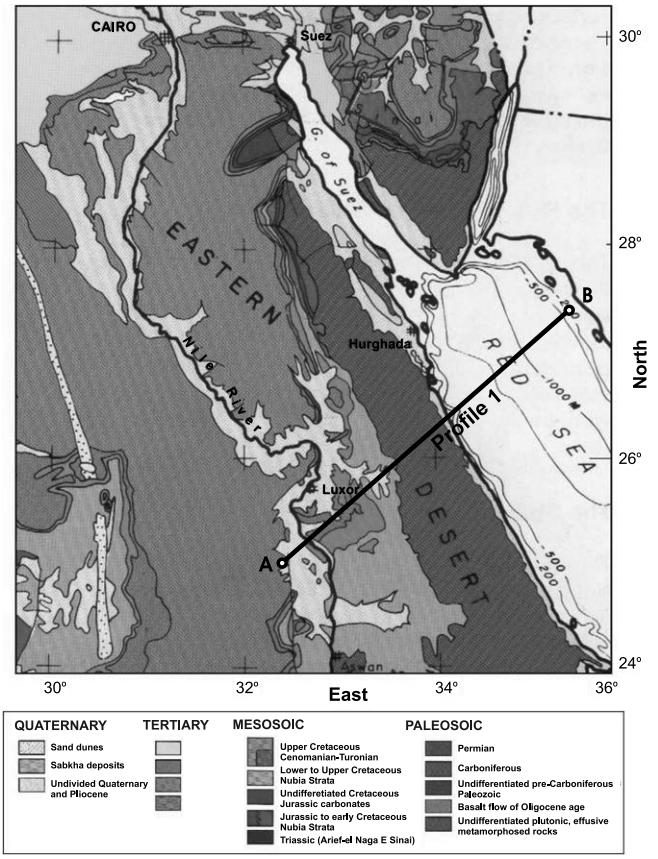

Fig. 1. Surface geological map for the region of study (from *Egyptian Geological Survey, 1994*) with location of studied profile.

time. The Cenozoic witnessed the transformation of the Tethys into the Mediterranean Sea. During the Palaeocene–Eocene, "deep sea conditions" migrated southwards and shallow water conditions of sedimentation or even land masses resulted in the northern part of Egypt, which now corresponds to the southern Mediterranean Sea. Thick calcareous deposits built by the Eocene limestones (the most widespread marine deposits in Egypt) are due to the deep sea evolution in the south. The limestones extend over the central part of Egypt where it constitutes a large plateau, crossed by the River Nile over a distance of 560 km, and in the central part of Sinai. The

Miocene was a period of great transformation, leading to the present Red Sea coast sediments and similar sedimentation in the north-western part of the Gulf of Suez *(Saleh et al., 2006)*. After the Oligocene uplift, an Early and Middle Miocene Tethys transgression began, only to be followed by late Miocene regression related to Alpine orogeny to the north. More extensive marine beds were formed in the Miocene, with a maximum extent in the Middle Miocene, when they reached to the Gulf of Suez and the Red Sea region beyond the Egyptian border. Pliocene sediments are widely distributed along the Red Sea. The Quaternary was characterized by regression with minor transgression. Uplift and tectonic disturbances mark the Pliocene-Quaternary boundary in the Red Sea region. Volcanism occurred in the Red Sea axial trough (*El-Gezeery and Marsouk, 1974; Saleh et al. 2006*).

3. Method

The integrated numerical modelling is based on 2D joint interpretation of thermal data, topography, geoid and gravity data to determine the lithosperic thermal structure in the study area. Since the relationship between surface heat flow values and geotherms in the deeper parts of the crust and in the upper mantle may be obscured by near-surface effects like groundwater flow or paleoclimatic variations, as well as by the generally unknown distribution of heat-producing elements in the crust, determinations of lithospheric thickness based only on surface heat flow data have large uncertainties. To reduce this uncertainty, we take into account the dependence of density on temperature through the coefficient of thermal expansion:

$$\rho\,(T) = \rho_0\,(1 - \alpha\,(T - T_0))\,,$$

where $\rho\,(T)$ is the density (kg/m^3) at a given temperature T ($^\circ$ C), ρ_0 is the density at temperature T_0 (usually room temperature except for the mantle, where it is given at asthenospheric temperature) and α is the thermal expansion coefficient taken as 3.5×10^{-5} K^{-1}.

We constrain in this way lateral temperature variations through their effect on geophysical observations that are influenced by the density distribution. The geophysical observable used for this, topography, gravity and geoid, have all different distance dependence on density variations.

The topography is calculated in local isostatic equilibrium using the formulas presented by *Lachenbruch and Morgan (1990)*:

$$h = \frac{\rho_a - \rho_L}{\rho_a} H + h_0,$$

with h topography (m), ρ_a asthenospheric density (3200 kg/m^3), ρ_L average lithospheric density (kg/m^3), calculated along columns based on the defined bodies (see description below), H thickness of the lithosphere (m), and h_0 calibration constant (-2380 m) that refers the obtained topography to average mid-oceanic ridge topography (*Lachenbruch and Morgan, 1990*).

If h becomes negative (labelled h_{neg}), one has to add the effect of water pressure:

$$h_{\text{neg}} = \frac{\rho_a}{\rho_a - \rho_{\text{water}}} h.$$

Topography is therefore sensitive to lateral variations of the average density above a certain compensation level. This level is defined within the asthenosphere that is supposed to have a sufficiently small viscosity to relax shear stresses at geologically short timescales and to have a constant density.

Gravity anomalies depend on distance r to density variations by r^{-2}. Therefore gravity anomalies will depend mainly on density variations within the crust with a relatively small, however not negligible, effect from density variations within the mantle. Gravity anomalies are calculated using a two-dimensional (2-D) algorithm (*Talwani et al., 1959*).

The geoid, reflecting variations of the elevation of the gravimetric isopotential surface corresponding to sea level depends on the distance to density variations by r^{-1}. The geoid is therefore more sensitive to near-surface density variations (specifically to topography) than to deep ones. However, the decay is relatively slow, and therefore geoid anomalies reflect crustal as well as mantle density variations. The formulas used have been published by *Zeyen et al. (2005)*.

The program used consists of a 2-D finite element algorithm to calculate the temperature distribution based on a user-defined lithospheric structure where each body is characterized by its density, thermal conductivity and heat production. The body structure is, as much as possible, constrained by existing seismic and geological data. The thermal boundary conditions are fixed temperatures at the upper limit (Earth's surface; 20° C) and the lower

one (lithosphere-asthenosphere boundary; 1300° C), as well as no horizontal heat flow at the lateral, vertical boundaries.

4. Geophysical data

Topography (Fig. 2a) was taken from the GTOPO30 database *(Gesch et al., 1999)*. Topography along Profile 1 in the Red Sea region is characterized by values of 0 to −1000 m. The uncertainty in determination of topography is about 25 m.

The free air gravity anomalies (Fig. 2b) were taken from the TOPEX 1-min gravity data set (`ftp://topex.ucsd.edu/pub` *(Sandwell and Smith, 1997)*). Values between −20 and 0 mGal with uncertainties of approximately 2 – 7 mGal are observed along Profile 1 in the Red Sea.

Geoid data (Fig. 3a) are taken from the EGM96 global model *(Lemoine et al., 1998)* with errors of less than 30 cm (`http://cddis.gsfc.nasa.gov/926/egm96/contents.html`). The Red Sea region has average geoid undulations of 12-13 m.

The surface heat flow density data (Fig. 3b) were compiled from the worldwide data set of *Pollack et al. (1993)*. Values between 80-150 mW m^{-2} were observed along Profile 1 in the Red Sea.

Moho depths were taken from Geological and geophysical information system for Eurasia, the Middle East and North Africa, digital database development for the Middle East and North Africa (`http://www.geo.cornell.edu/geology/me_na/report/report.html`).

5. Results

The initial model was compiled after a 3D gravity model calculated by IGMAS by *Saleh et al. (2006)*. The thermal and density-related parameters were then modified by the method of trial-and-error until a reasonable fit was obtained between the data and model predictions. Densities and thermal properties of the different bodies used in the resultant model of Profile 1 (Fig. 4) are illustrated in Table 1.

From the resultant integrated lithospheric crossection along Profile 1, (Fig. 4) the following can be observed:

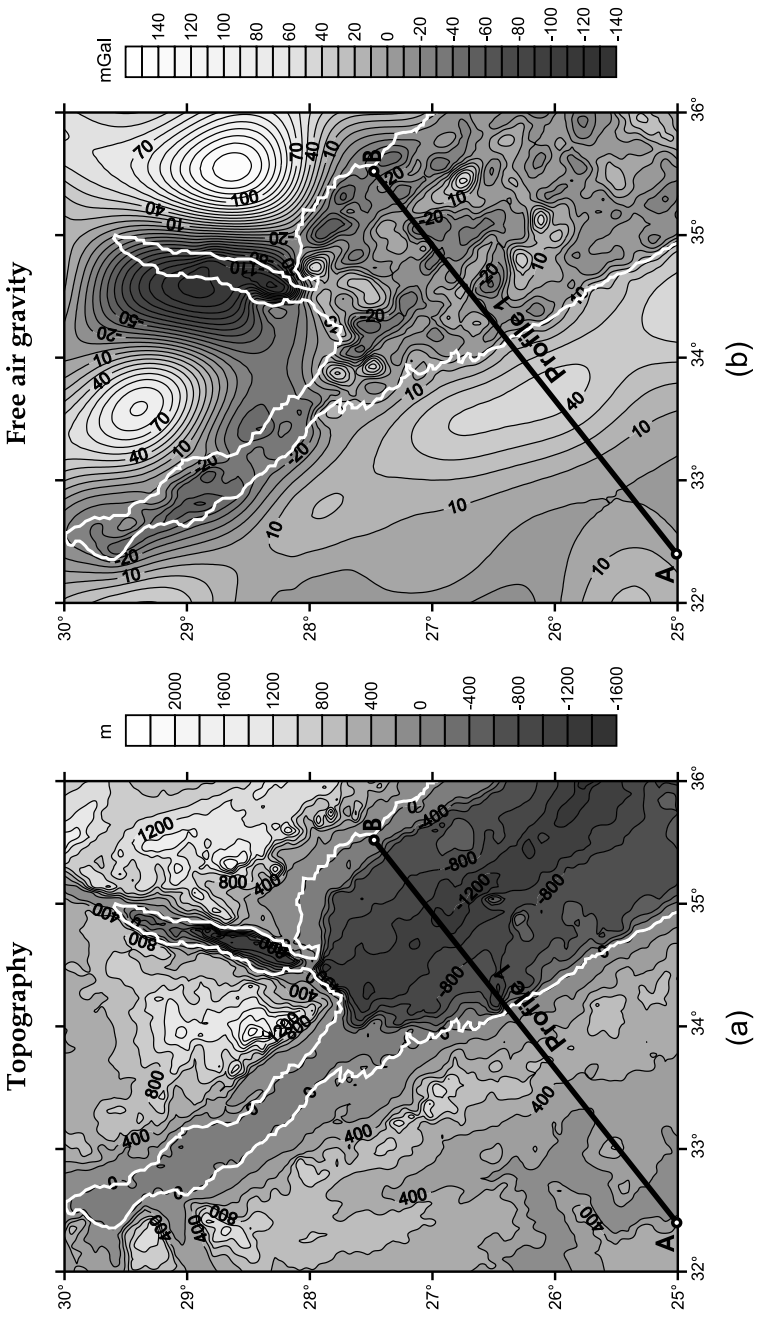

Fig. 2. (a) Topography of the Red Sea region (from GTOPO30 data set *(Gesch et al., 1999)*). (b) Smoothed free-air gravity anomaly map of the Red Sea region (from TOPEX gravity data, 1 min grid, `ftp://topex.ucsd.edu/pub`).

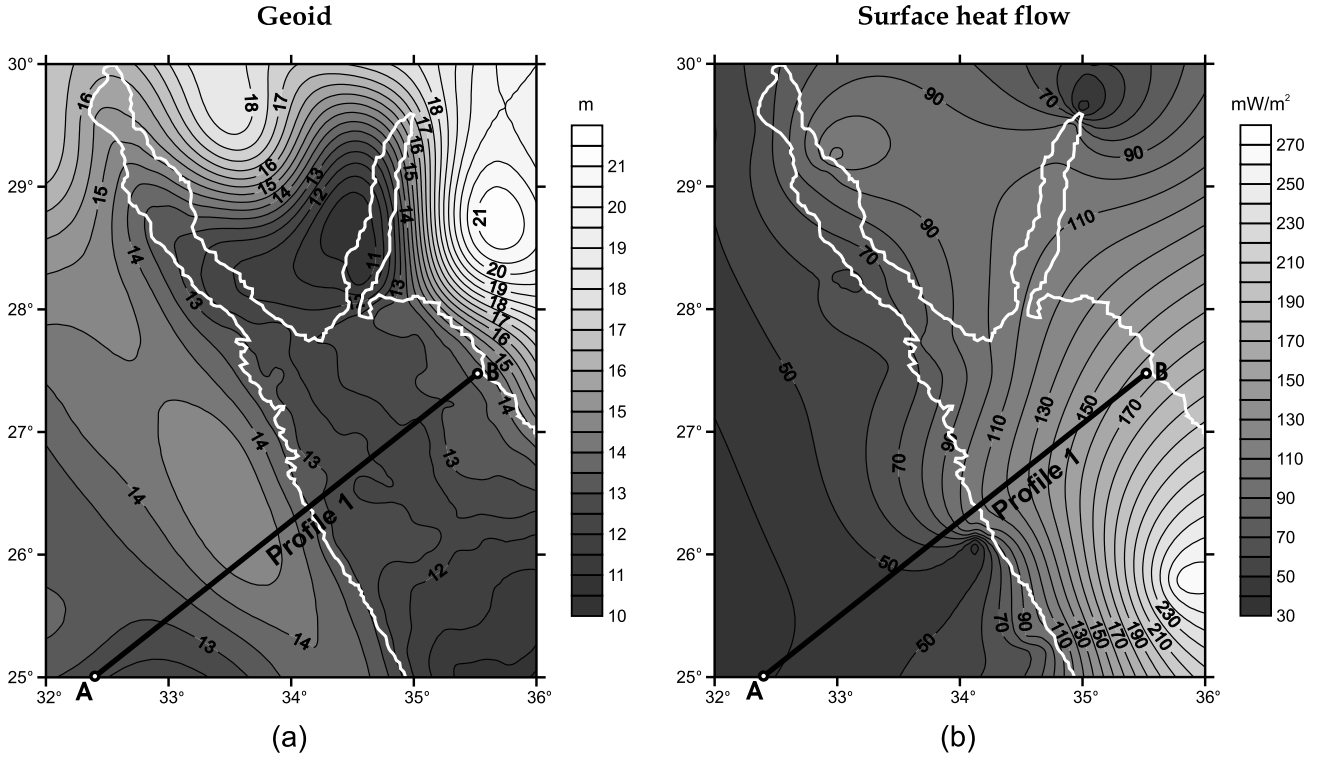

Fig. 3. (a) Geoid anomaly map of the Red Sea region (from TOPEX geoid data, 2 min grid, `ftp://topex.ucsd.edu/pub`). (b) Map of the surface heat flow density of the Red Sea region (from *Pollack et al., 1993*).

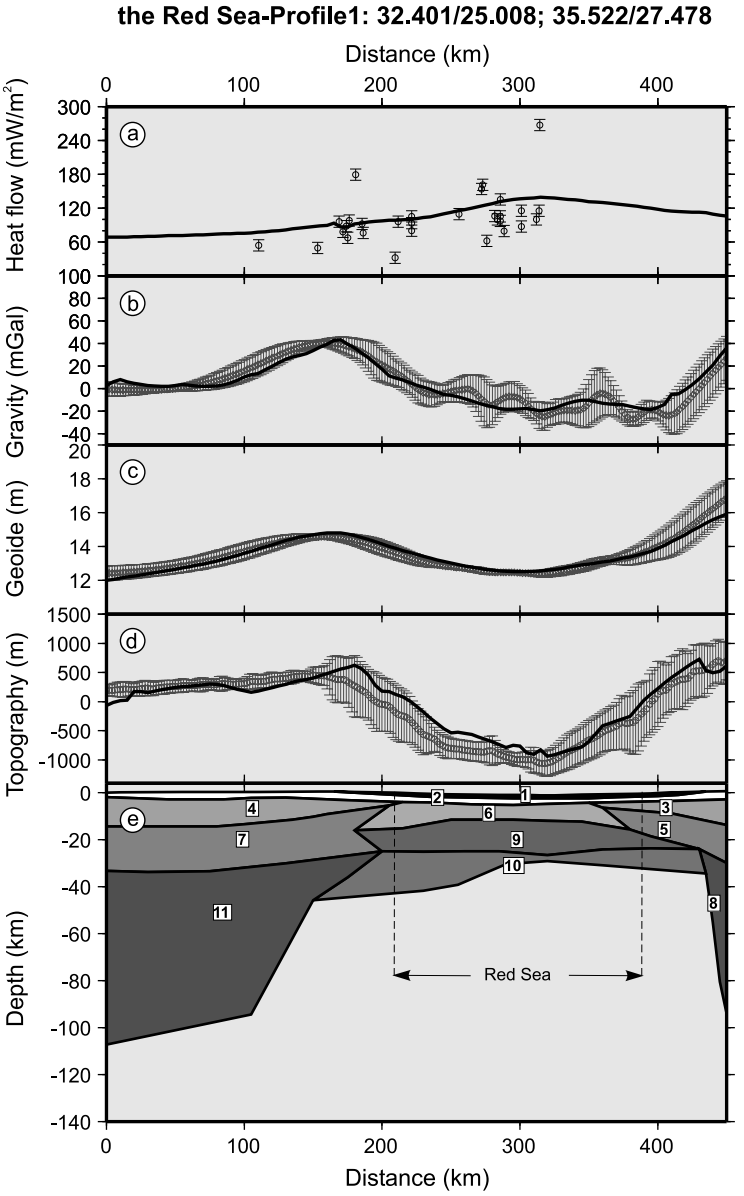

Fig. 4. Lithospheric model along Profile 1 (with exact coordinates) (a) surface heat flow, (b) free-air gravity anomaly, (c) geoid, (d) topography with dots corresponding to measured data with uncertainty bars and solid lines to calculated values, (e) lithospheric structures. Numbers within the model bodies correspond to material number in Table 1.

Table 1. Densities and thermal properties of the different bodies used in the resultant model of Profile 1

Nr.	Unit	HP	TC	ρ_0
1	Quaternary and Pliocene sediments	3.0	2.5	2220
2	Tertiary sediments	3.0	2.5	2400
3, 4	Upper crust (basement rocks)	2.0	2.0	2750
6	Igneous crust	0.2	2.0	2850
5, 7	Lower crust	0.2	2.0	2900
8, 11	Normal upper mantle	0.05	3.4	3250
9	Red Sea upper mantle	0.05	3.4	3200
10	Red Sea anomalous upper mantle	0.05	3.4	3120

Nr.: Reference number in Fig. 4;
HP: Heat production ($\mu W/m^3$);
TC: Thermal conductivity (W/(m K));
ρ_0: density at room temperature (kg/m^3).

– The depth of the Quaternary and Pliocene sediments underneath the Red Sea varies from 1 km to 2.4 km (see Fig. 4). Beneath this layer, the Tertiary sedimentary basement is located up to the depth of 5 km.
– On the Red Sea coast, the crust is continental, about 28-33 km thick, shallowing towards the Red Sea area. Underneath the Red Sea, an igneous oceanic crust with thickness that ranges from 12 to 15 km can be found.
– The lithosphere-asthenosphere boundary was modelled at the depths from about 30 km to 45 km beneath the Red Sea. The lithospheric thickness in the area of the Red Sea is much thinner than the continental one that was modelled at the depths of 100-120 km. To obtain a reasonable fit between the observed and calculated data, it was necessary to add a low density anomalous body to the lowermost part of the Red Sea upper mantle.

6. Conclusions

The density model shows clear large differences in the crustal and lithospheric thickness between continental and oceanic parts of the model. The oceanic crust of the Red Sea is much thinner (12-15 km) compared to the continental crust which is located on both sides of the Read Sea. The continental crust located the eastward (westward) from the Read Sea reaches the thickness of about 28-33 km. The low density anomalous body located

in the lowermost part of the upper mantle in the Red Sea area indicates the possible presence of partial melting in the upper mantle and supports the idea that a large scale asthenospheric upwelling might be responsible for the subsequent rifting of the Red Sea. The uplift of the asthenospheric mass in the Read Sea could be accompanied by the process of underplating beneath the Moho discontinuity. This result is in good agreement with results published by *Makris et al. (1988)*, *Makris and Ginzburg (1987)* and *Martinez and Cochran (1988)*.

Acknowledgments. Bielik, Dérerová and Kohút are grateful to the Science and Technology Assistance Agency under the contract No. APVT-51-002804. This work was also supported by the Slovak Grant Agency VEGA (grants No. 1/3066/06 and 2/6019/06). Authors are grateful to Prof. Hermann Zeyen of University de la Terre for permission to use 2D integrated modelling software.

References

Egyptian Geological Survey, 1994: Geological map of Sinai, Arab Republic of Egypt, Scale 1:250 000.

El-Gezeery M. V., Marsouk I. M., 1974: Miocene rock stratigraphy of Egypt. Egypt. J. Geol., **18**, 1–59.

Gaulier J. M., Le Pichon X., Lyberis N., Avedik F., Geli L., Moretti I., Deschamps A., Salah, Hafez, 1988: Seismic study of the crust of the northern Red Sea and Gulf of Suez. Tectonophysics, **153**, 55–88.

Gesch D. B., Verdin K. L., Greenlee S. K., 1999: New land surface digital elevation model covers the Earth, Eos Trans. AGU, **80**, 69–70.

Lachenbruch A. H., Morgan P., 1990: Continental extension, magmatism and elevation; formal relations and rules of thumb. Tectonophysics, **174**, 39–62.

Lemoine F. G., Kenyon S. C., Factor J. K., Trimmer R. G., Pavlis N. K., Chinn D. S., Cox C. M., Klosko S. M., Luthcke S. B., Torrence M. H., Wang Y. M, Williamson R. G., Pavlis E. C., Rapp R. H., Olson T. R., 1998: The Development of the Joint NASA GSFC and the NIMA Geopotential Model EGM96, NASA TP/-1998-206861, NASA Goddard Space Flight Center, 575 pp.

Makris J., Allam A., Moktar T., Basahel A., Dehghani G. A., Bazari M., 1983: Crustal structure at the northwestern region of the Arabian shield and its transition to the Red Sea. Bull. Fac. Earth Sci. K. Abdulaziz Univ., **6**, 435–447.

Makris J., Ginzburg A., 1987: The afar depression: transition between continental rifting and sea-floor spreading. Tectonophysics, **141**, 199–214.

Makris J., Rihm R., Allam A., 1988: Some Geophysical aspects of the evolution and structure of the crust in Egypt. In: Greiling, S.E.-G.a. R.O. (Ed.), The Pan-African Belt of Northeast Africa and Adjacent Areas, Tectonic Evolution and Economic Aspects of a Late Proterozoic Orogen: Braunschweig, Friedr. Vieweg & Sohn, 345–369.

Martinez F., Cochran J. R., 1988: Structure and tectonics of the northern Red Sea: catching a continental margin between rifting and drifting. Tectonophysics, **150**, 1–32.

Pollack H. N., Hurter S. J., Johnson J. R., 1993: Heat flow from the Earth's interior: Analysis of the global data set. Rev. Geophys., **31**, 267–280.

Said R., 1962: The Geology of Egypt. Elsevier Publ. Co. Amsterdam and New York.

Saleh S., Jahr T., Jentzsch G., Saleh A., Abou Ashour N. M., 2006: Crustal evaluation of the northern Red Sea rift and Gulf of Suez, Egypt from geophysical data: 3-dimensional modelling. Journal of African Earth Sciences, **45**, 257–278.

Sandwell D. T., Smith W. H. F., 1997: Marine gravity anomalies from Geosat and ERS-1 satellite altimetry. J. Geophys. Res., **102**, 10039–10054.

Talwani M., Worzel J. L, Landisman M., 1959: Rapid gravity computations for two-dimensional bodies with application to the Mendocino submarine fracture zone. J. Geophys. Res., **64**, 49–59.

Tramontini C., Davies D., 1969: A seismic refraction survey in the Red Sea. Geophys. J. R. Astron. Soc., **17**, 2225–2241.

Zeyen H., Ayarza P., Fernàndez M., Rimi A., 2005: Lithospheric structure under the western African-European plate boundary: A transect across the Atlas Mountains and the Gulf of Cadiz. Tectonics, **24**, TC2001, doi:10.1029/2004TC001639.